Mitochondrial Communications 2 (2024) 14–20

Contents lists available at ScienceDirect

Mitochondrial Communications

journal homepage: www.keaipublishing.com/en/journals/mitochondrial-communications

Research Article

Mitochondrial calcium transport during autophagy initiation

Sujyoti Chandra, Parul Katiyar, Aarooran S. Durairaj, Xinnan Wang *

Department of Neurosurgery, Stanford University School of Medicine, Stanford, CA94305, USA

ARTICLE INFO

Keywords:
Mitochondrial Ca^{2+} uptake
Mitophagy
Autophagy
ER Ca^{2+} transient
Parkinson
MCU
IP3R
RyR

ABSTRACT

While it has been shown that Ca^{2+} dynamics at the ER membrane is essential for the initiation of certain types of autophagy such as starvation-induced autophagy, how mitochondrial Ca^{2+} transport changes during the first stage of autophagy is not systemically characterized. An investigation of mitochondrial Ca^{2+} dynamics during autophagy initiation may help us determine the relationship between autophagy and mitochondrial Ca^{2+} fluxes. Here we examine acute mitochondrial and ER calcium responses to a panel of autophagy inducers in different cell types. Mitochondrial Ca^{2+} transport and Ca^{2+} transients at the ER membrane are triggered by different autophagy inducers. The mitophagy-inducer-initiated mitochondrial Ca^{2+} uptake relies on mitochondrial calcium uniporter and may decelerate the following mitophagy. In neurons derived from a Parkinson's patient, mitophagy-inducer-triggered mitochondrial Ca^{2+} influx is faster, which may slow the ensuing mitophagy.

1. Introduction

Ca^{2+} ions travel in and out of the cells and organelles and cause dynamic changes in Ca^{2+} concentrations and transients across subcellular domains, which could serve signals to control diverse cellular functions and processes.[1] For example, autophagy is known to require intracellular and ER Ca^{2+} signaling.[1–4] Mitochondria are one of the cellular Ca^{2+} reservoirs and mitochondria Ca^{2+} homeostasis plays a crucial role in health and disease.[5–10] Intracellular Ca^{2+} can be imported into the mitochondria through the outer mitochondrial membrane (OMM) channel, VDAC, and the inner mitochondrial membrane (IMM) channel, mitochondrial calcium uniporter (MCU).[11] Mitochondrial Ca^{2+} can be exported to the cytosol via the IMM transporter, NCLX.[12] Mitochondria can acutely take up cytosolic Ca^{2+} to buffer intracellular Ca^{2+}-level elevation, which could occur during neuronal firing or when other organelles release their Ca^{2+} to the cytosol. Whether acute mitochondrial uptake of Ca^{2+} plays a signaling role in distinct cellular processes remains elusive. Mitochondrial Ca^{2+} mishandling and mitophagy (mitochondria-specific autophagy) impairment have been found in neurodegenerative diseases such as Parkinson's disease (PD),[5–10,13–17] but the link between Ca^{2+} and mitophagy is under explored. Here we live monitor mitochondrial and ER Ca^{2+} transport immediately following autophagy induction in human non-neuron cells and neurons and dissect the relationship between mitochondrial Ca^{2+} and mitophagy.

2. Materials and methods

2.1. Constructs

pcDNA3.1-ER-GCaMP6f was a gift from Chris Richards (Addgene#182548). pCMV-R-CEPIA1er was a gift from Masamitsu Iino (Addgene#58216). pCMV-Mito4x-GCaMP6f was a gift from Timothy Ryan (Addgene#127870). pHAGE-mt-mkeima was a gift from Richard Youle (Addgene#131626). pDsRed2-Mito was described in.[17]

2.2. Cell culture

HEK293T cells were cultured in DMEM media (11995-073, Gibco) supplemented with 10 % FBS (35011CV, Corning) and 1 % Penn-Strep (15140122, Gibco) and maintained in a 37 °C, 5 % CO_2 incubator with humidified atmosphere. Once cells reach 80 % confluency, they were dissociated using Trypsin-EDTA (25200056, Gibco) and seeded into a new flask. Cells were treated with 500 μM Cobalt Chloride for 18 h, 1 μM RU360 (557440, Sigma-Aldrich) for 24 h, 100 μM 2-APB (1224, Tocris) for 1 h, or 100 μM Ryanodine (1329, Tocris) for 1 h. Induced pluripotent stem cells (iPSCs) were obtained from NINDS (PD-SNCA-A53T, ND50050; Isogenic-WT, ND50085; 51y, Female). iPSCs were differentiated into midbrain dopaminergic neurons using an adaptation of the dual-SMAD inhibition method as previously described.[15,17–21] The percent of Tyrosine Hydroxylase (TH) positive neurons were quantified as in.[16]

* Corresponding author.
E-mail address: xinnanw@stanford.edu (X. Wang).

https://doi.org/10.1016/j.mitoco.2024.01.002
Received 23 November 2023; Received in revised form 16 January 2024; Accepted 26 January 2024
Available online 28 January 2024

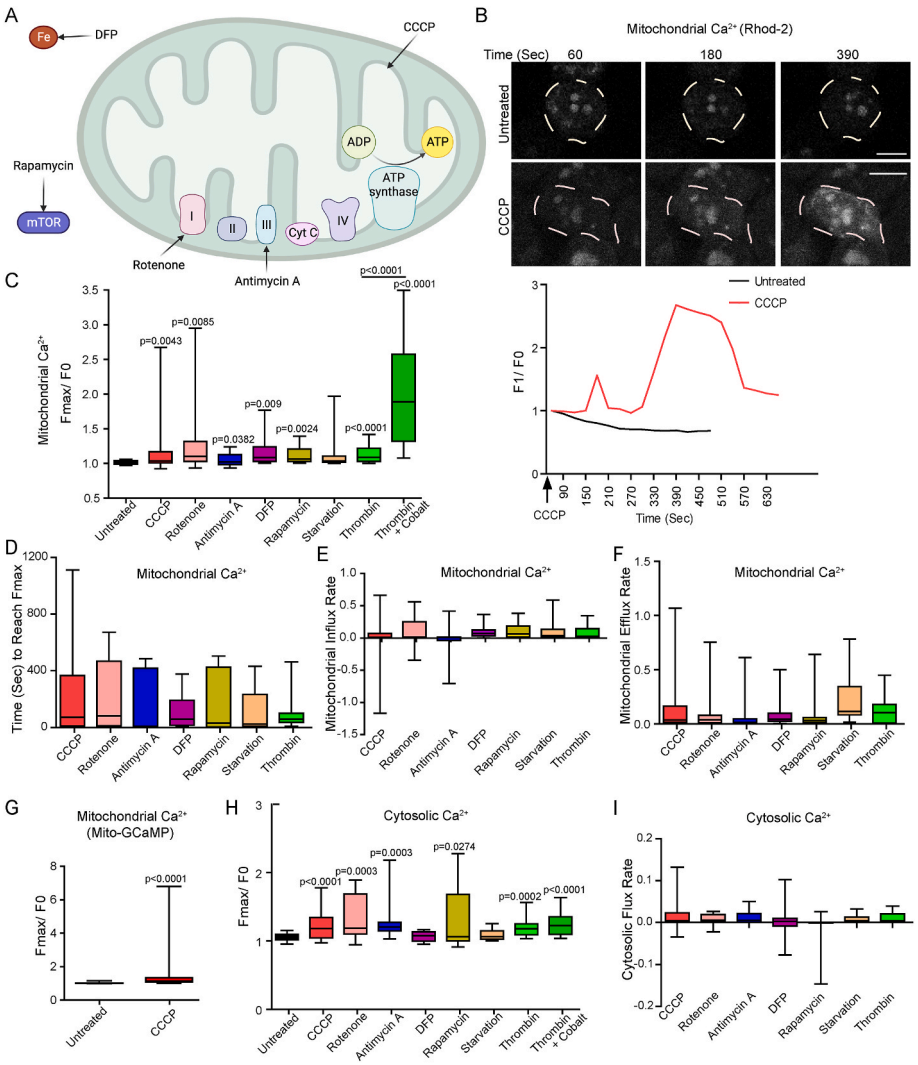

Fig. 1. Mitochondrial and cytosolic Ca^{2+} changes during autophagy initiation in HEK cells. (A) Schematic representation of different autophagy inducers and their targets. (B) Representative time-lapse images and traces of Rhod-2 staining. Scale bars: 10 μm. (C–F) Rhod-2 quantifications. (C) Fmax/F0. (D) Time to reach Fmax. (E) Influx rate. (F) Efflux rate. (G) Fmax/F0 detected by Mito-GCaMP6f. (H–I) Calcium Green quantifications. (H) Fmax/F0. (I) Flux rate. (C, H) Two-tailed Welch's T-Test. Compared with "untreated", except labeled. (D, E, F, I) One-Way Anova Post Hoc Tukey Test. (G) Mann Whitney Test. n = 15–42 cells from 3 to 8 coverslips.

2.3. Transfection

Cells grown for 24 h on glass coverslips in a 24-well plate were co-transfected with ER-GCaMP6f and ER-CEPIA (1:1 ratio; 0.6 μg each) and 1–2 μl Lipofectamine 2000 (11668-030, Invitrogen) or polyethyenimine (PEI; 49553-93-7, Polysciences) following manufacturer's protocols. The next morning, media was replaced with fresh DMEM. Cells were used for experiments 48 h post-transfection.

2.4. Western blotting and immunocytochemistry

Same as in[17] and.[16] Anti-LC3 (2775S, Cell Signaling) was used at 1:1000.

2.5. Live cell imaging

Rhod-2 (R1244, Thermo Fisher) and Calcium Green (C3011MP, Thermo Fisher) at 5 μM were applied to cells on coverslips in culture media and incubated at 37 °C for 30 min, then coverslips were washed with PBS and each was placed in a 35-mm petri-dish containing Hibernate E low-fluorescence medium (BrainBits/Transnetyx), and cells were imaged immediately on a heated stage of 37 °C with a 63/N.A.0.9 water-immersion objective. Time-lapse movies were obtained continually with a 2–30 s interval for 10–20 min. During imaging, the following drugs were added: 40 μM CCCP (C2759, Sigma-Aldrich), 10 μM Rotenone (HY–B1756, MedChemExpress), 10 (HEK cells) or 100 μM (neurons) Antimycin A (A8674, Sigma-Aldrich), 1 mM DFP (HY–B0568, MedChemExpress), 1 μM Rapamycin (HY-10219, MedChemExpress), or 100 mUnits/ml Thrombin (10602400001, Sigma-Aldrich).[17] For starvation, after a 30-min incubation with dyes in media, the coverslip was transferred in HBSS (14025, Gibco) and imaged immediately. MitoNeoD at 5 μM (563761, MedKoo Biosciences Inc.), MitoTracker Green at 75 nM (M7514, Thermo Fisher), or TMRM at 25 nM (T668, Molecular Probes) was applied to cells on coverslips in media at 37 °C for 30 min and imaged with the same set-up as above. Mito-dsRed imaging was described in.[17]

2.6. Image analysis

The fluorescence intensity when the inducer was administered was considered as F0. After F0, the peak fluorescent intensity was considered as Fmax and Fmax/F0 was calculated. The influx rate = [(Fmax-F0)/T]

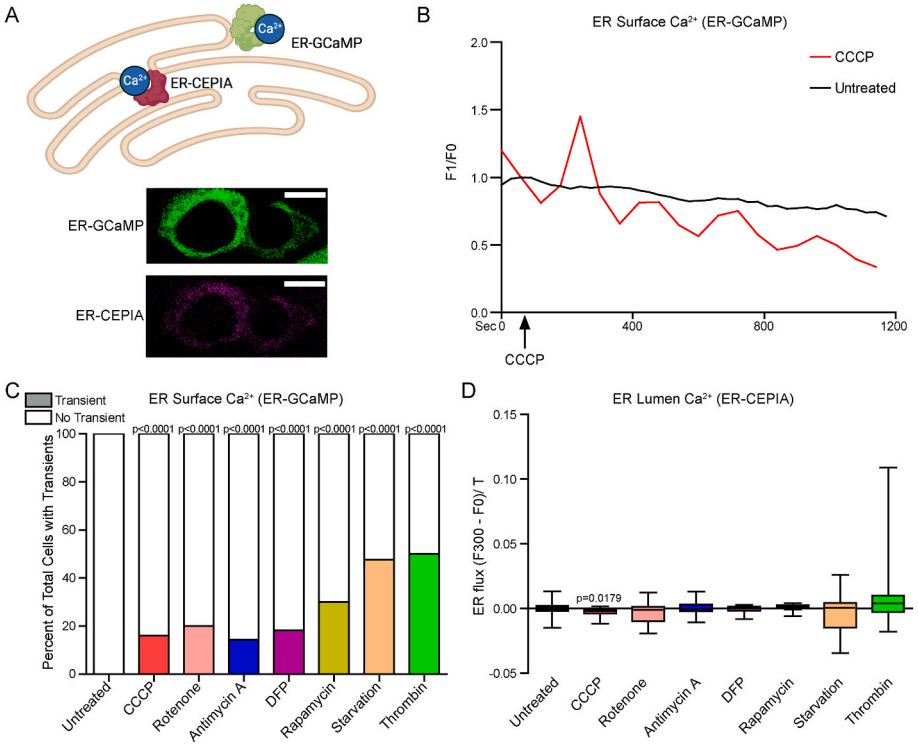

Fig. 2. ER Ca^{2+} changes during autophagy initiation in HEK cells. (A) Scheme (upper) and representative images (lower) of ER-GCaMP6f (ER surface) and ER-CEPIA (ER lumen). Scale bars: 10 μm. (B) Representative traces of ER-GCaMP6f. (C) The percentage of cells displaying calcium transients detected by ER-GCaMP6f. Chi-Square Test. (D) ER flux rate detected by ER-CEPIA. One-Way Anova Post Hoc Tukey Test. (C–D) n = 21–35 cells from 3 to 5 coverslips.

(T, time to reach Fmax). The efflux rate = [(Fmax-F′)/T' (F′ is the fluorescent intensity after Fmax closest to F0; T′, time from Fmax to F'). The percentage of cells that showed ER-GCaMP6f trace oscillation (at least one F1/F0 peak>1.4) was calculated. The ER-CEPIA flux rate = [(F300–F0)/300].

2.7. Seahorse analysis

Cells were seeded into an XF HS Mini cell culture miniplate at a density of 2.0×10^4 cells/well. The two edge wells were filled with only media to serve as background controls. After overnight recovery in a 37 °C, 5 % CO_2 incubator, cells were washed with 200 μl/well of fresh XF DMEM pH 7.4 (Agilent Technologies) and incubated with 200 μl/well fresh XF DMEM supplemented with glucose (10 mM), pyruvate (1 mM), and glutamine (2 mM) in a 37 °C, non-CO_2 incubator for 1 h. Prior to starting the assay, the assay medium was removed and replaced with 180 μl/well of fresh medium with supplements. The miniplate was then loaded into a Seahorse XF HS Mini Analyzer (Agilent Technologies) with temperature set at 37 °C. Samples were treated with 1.5 μM Oligomycin (complex V inhibitor) and 0.5 μM Rotenone plus 0.5 μM Antimycin A (complex I & III inhibitor). A total of three measurements were taken after each compound was administered. After completion of the Seahorse assay, each well was lysed with an in-house lysis buffer (1 % Triton, 50 mM Tris pH 7.5, 300 mM NaCl, 0.1 % protease inhibitor cocktail, 0.2 mM PMSF) and quantified for the total protein amount with a Bicinchoninic acid (BCA) assay (Thermo Scientific) for normalization.

2.8. Growth curve assay

Cells were seeded into a 24-well plate at a density of 5.0×10^3 cells/well, trypsinized with 0.25 % Trypsin-EDTA each day after seeding, and counted using a TC20 Automated Cell Counter (BioRad). The initial seeding density was used as the cell count for day 0.

2.9. Mitophagy assay

Cells were plated in a 96-well assay plate (black with clear flat bottom) (Corning, 3340) and grown for 24 h followed by transfection with 0.1 μg of Mito-mKeima using PEI. Cells were treated with 40 μM CCCP for the following duration: 24, 12, or 6 h. Two days post-transfection and immediately after treatments, the plate was read using a TECAN plate reader with excitation wavelength between 400 and 594 nm (step size of 2 nm) and emission wavelength at 620 nm. The fluorescence ratio at 586/440 nm was calculated and normalized to 0 h within each group.

2.10. Graphics

Created with BioRender.com.

3. Results

3.1. Mitochondrial calcium transport is triggered by autophagy inducers

We live recorded cytosolic and mitochondrial Ca^{2+} levels in HEK293T cells with Calcium Green and Rhod-2 staining, respectively,[17] immediately following the addition of a panel of autophagy inducers (Fig. 1A and B). We included the following inducers: starvation (autophagy),[1] Rapamycin (autophagy by inhibiting mTOR),[3] DFP (autophagy by chelating iron),[22] Rotenone (autophagy by inhibiting the complex I),[23,24] Antimycin A (mitophagy by inhibiting the complex III[14–16]), and CCCP (mitophagy by depolarizing the membrane potential).[25] Thrombin, a G-protein-coupled receptor (GPCR) agonist shown to stimulate cytosolic Ca^{2+} elevation and mitochondrial Ca^{2+} uptake via MCU,[26,27] was used as a positive control. We found thrombin treatment caused an immediate increase in the Calcium Green and Rhod-2 intensities (Fig. 1C–F, H-I), consistent with previous studies.[17,26,27] In addition, pretreatment of the cells with Co^{2+} for 24 h further boosted mitochondrial Ca^{2+} uptake upon thrombin treatment (Fig. 1C), in

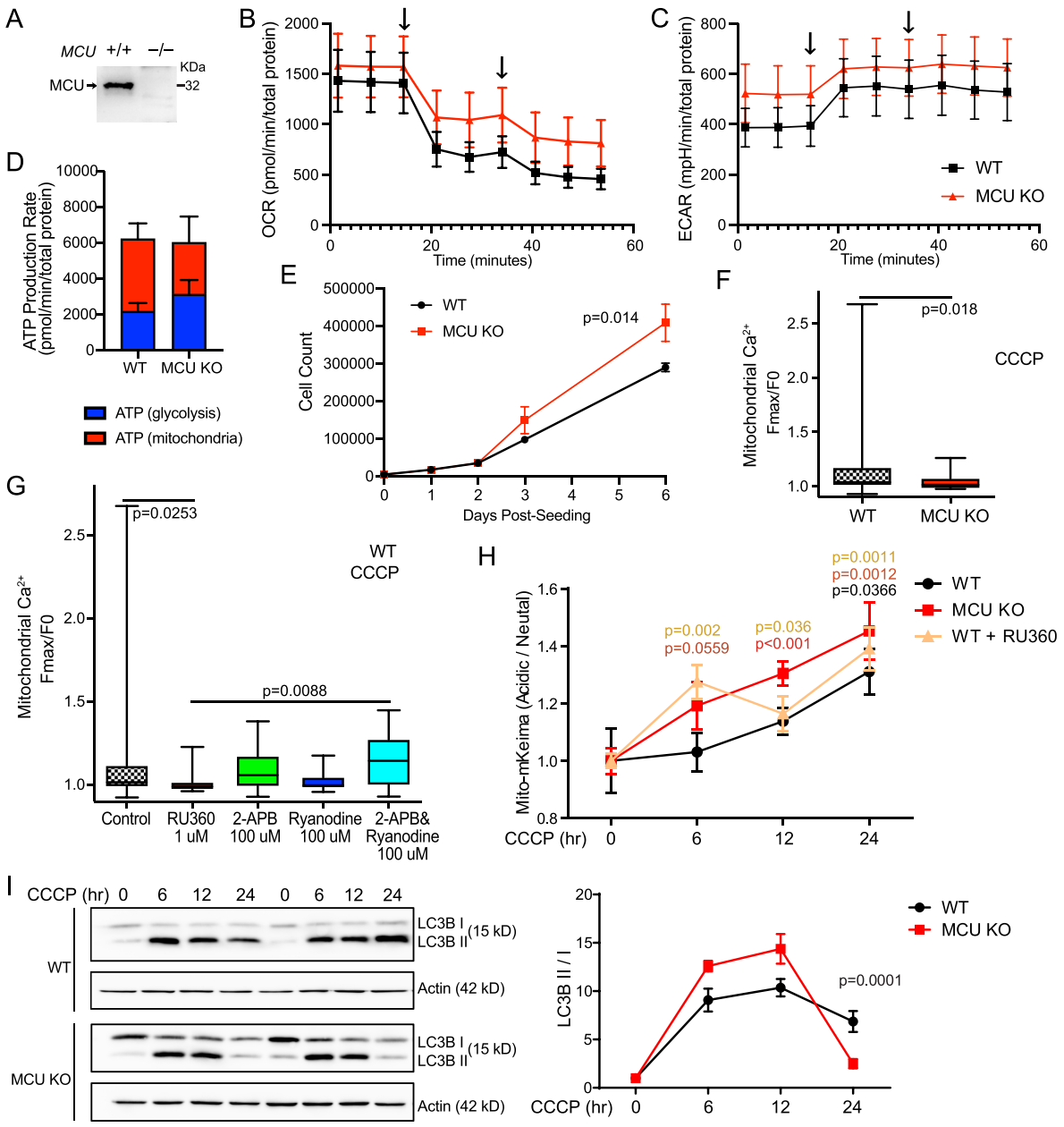

Fig. 3. Mitophagy-triggered mitochondrial Ca^{2+} uptake requires MCU and MCU inhibition accelerates mitophagy. (A) Lysates as indicated were blotted with anti-MCU. (B–D) Seahorse analysis. Each OCR or ECAR value was from one well of a miniplate. n = 3 wells. Black arrows show the times of Oligomycin and Rotenone/Antimycin A injections. (E) Growth curves. (B–E) n = 3. (F–G) Rhod-2 quantifications of Fmax/F0 in cells with indicated genotypes and treatments. (F) n = 18–42 cells from 3 to 8 coverslips. (G) RU360 for 24 h, 2-APB and Ryanodine for 1 h n = 30–78 cells from 3 to 11 coverslips. (H) The ratio of Mito-mKeima is plotted. n = 8–12. (I) Lysates of indicated genotypes and treatments were immunoblotted. The ratio of the intensity of LC3BII/I was calculated. n = 4. (B-E, H–I) Mean ± SEM. (E, I) Two-Way Anova. (F, H) Two-tailed Welch's T-Test. Compared with the left bar. (G) One-Way Anova Post Hoc Tukey Test.

agreement with our previous finding showing that Co^{2+} binds to MCU to enhance MCU channel activity.[17] We discovered that all autophagy inducers tested, except starvation, caused a significant increase in the maximum mitochondrial Ca^{2+} uptake (Fmax/F0) compared to untreated controls (Fig. 1C), indicating that mitochondrial Ca^{2+} import is triggered. The time to reach Fmax (Fig. 1D), the mitochondrial Ca^{2+} influx rate (Fig. 1E), or the efflux rate (Fig. 1F) was comparable among different inducers. We verified our observation of Rhod-2 staining with a genetically encoded fluorescent Ca^{2+} indicator located in the mitochondrial matrix, Mito-GCaMP6f[28] (Fig. 1G). Cytosolic Ca^{2+} levels were also elevated upon the treatment of selective autophagy inducers (Fig. 1H and I). Together, our results show mitochondrial Ca^{2+} uptake is triggered during autophagy initiation.

3.2. Calcium concentration starts to oscillate at the ER membrane upon autophagy induction

We next live recorded Ca^{2+} dynamics at the ER membrane facing the cytosol using ER-GCaMP6f[29] and in the ER lumen using ER-CERPIA[30] (Fig. 2A), following the addition of autophagy inducers. We found that autophagy inducers caused Ca^{2+} concentrations to immediately fluctuate at the cytosolic face of the ER membrane (Fig. 2B and C), consistent with previous findings of starvation-induced autophagy.[1] Ca^{2+} concentrations in the ER lumen were either increased or decreased by different inducers, although most of the changes were nominal (Fig. 2D). These data show ER Ca^{2+} dynamic changes during autophagy initiation.

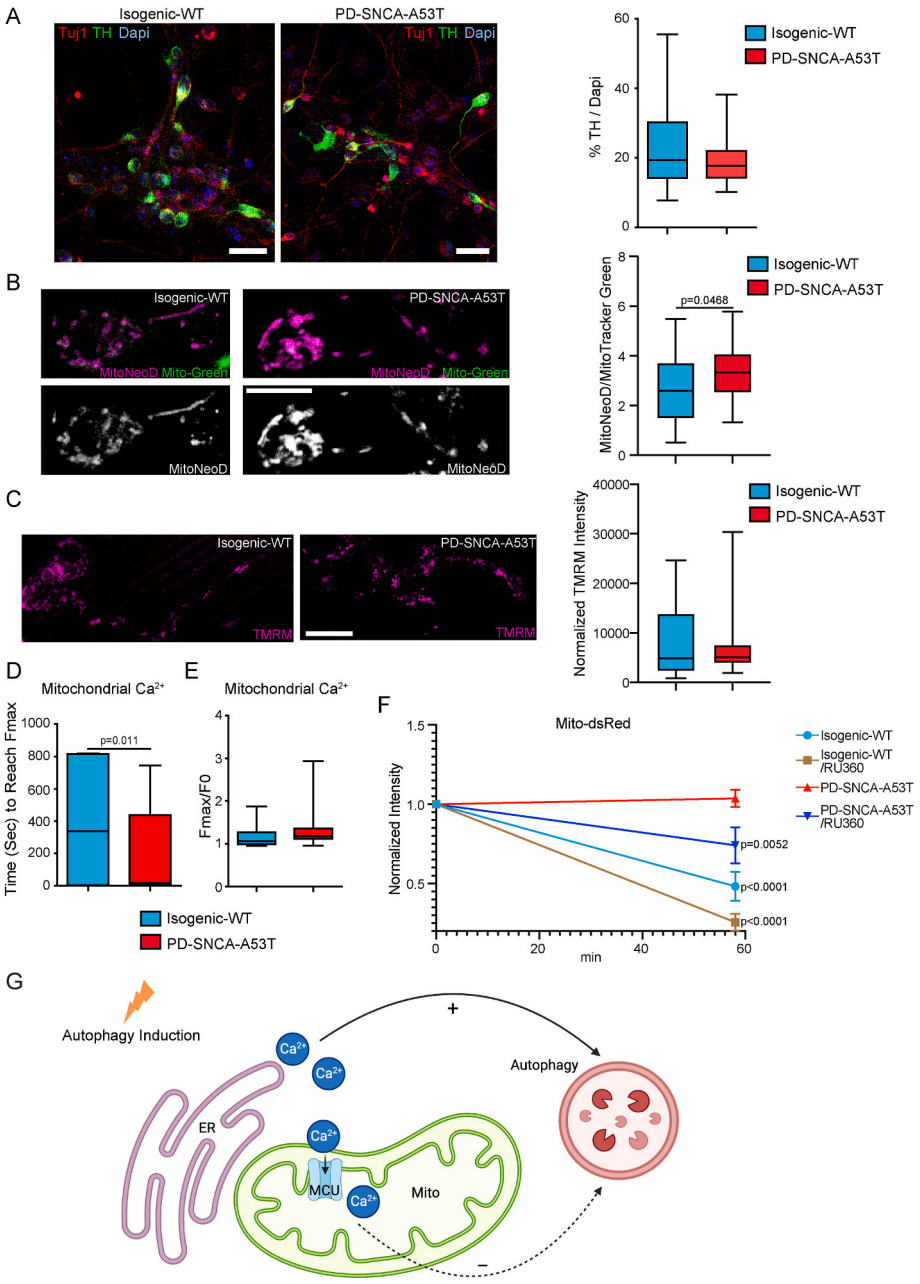

Fig. 4. Mitophagy-triggered mitochondrial Ca^{2+} uptake in iPSC-derived neurons. (A) Representative images and the percentage of TH-positive neurons (day 40). n = 30 images from 3 coverslips. (B) Left: Confocal single section images of live neurons stained with MitoNeoD and MitoTracker Green (Mito-Green). Right: Quantifications of the MitoNeoD fluorescent intensity normalized to MitoTracker Green. n = 25 cell bodies from 3 coverslips. (C) Left: Confocal single section images of live neurons stained with TMRM. Right: Quantifications of the TMRM fluorescent intensity subtracting the background. n = 20 cell bodies from 3 coverslips. Scale bars: (A) 20 μm; (B–C) 10 μm. (D–E) Rhod-2 quantifications. n = 29–30 from 3 coverslips. (A–E) Two-tailed Welch's T-Test. (F) As shown in,[17] images from live recordings of axons, following 100 μM Antimycin A treatment, were analyzed for calculating degradation rate profiles of Mito-dsRed, normalized to the same axonal region at 0 min n = 3 axons (one axon per coverslip). Comparison with "0 min". One-Way Anova Post Hoc Dunnett's Test. RU360 was applied at 1 μM for 24 h. (G) Schematic representation of this study.

3.3. *Mitophagy-inducer-triggered mitochondrial calcium uptake depends on MCU*

We reasoned that mitochondrial Ca^{2+} influx during autophagy required MCU, the main mitochondrial Ca^{2+}-uptake channel. To explore this possibility, we live recorded mitochondrial Ca^{2+} levels in HEK293T cells without endogenous MCU (MCU KO) or treated with an MCU inhibitor (RU360).[31] We validated MCU KO cells with anti-MCU (Fig. 3A). These MCU KO cells showed a slight, but insignificant increase in the oxygen consumption rate (OCR), extracellular acidic rate (ECAR), and glycolytic ATP production (Fig. 3B–D). These MCU KO cells also grew faster than wild-type cells (Fig. 3E), consistent with previous studies.[32] By live imaging Rhod-2 in these cells we found that CCCP-triggered mitochondrial Ca^{2+} uptake was significantly abolished (Fig. 3F). Similarly, inhibiting MCU with RU360 diminished mitochondrial Ca^{2+} influx following CCCP treatment (Fig. 3G). These findings show that MCU is required for mitophagy-inducer-triggered mitochondrial Ca^{2+} import.

To reveal whether ER provided Ca^{2+} ions that were imported into the mitochondria during mitophagy initiation, we applied 2-APB or Ryanodine, an inhibitor of IP3R or RyR, respectively.[5] IP3R and RyR are the

main ER Ca^{2+}-export channels. We discovered that CCCP-induced mitochondrial Ca^{2+} uptake was not significantly affected by 2-APB or Ryanodine, individually or combined, but was different between RU360 and combined 2-APB and Ryanodine treatment (Fig. 3G). Hence, it is possible that ER is not the only source that supplies Ca^{2+} to the mitochondria or Ca^{2+} is exported via non-IP3R/RyR channels during mitophagy.

3.4. Loss of MCU accelerates mitophagy

Next, we determined the role of mitochondrial Ca^{2+} uptake for mitophagy. We compared the mitophagy kinetics between wild-type (WT) and MCU KO HEK293T cells where mitochondrial Ca^{2+} uptake during mitophagy was prevented (Fig. 3F), by using the ratiometric mitophagy reporter, Mito-mKeima.[15,16] An increase in the ratio of the 586 to 440 nm (excitation) intensity of Mito-mKeima indicates an increase in lysosome fusion with mitochondria-containing autophagosomes. We found that in MCU KO cells it took less time to raise the ratio of Mito-mKeima following CCCP treatment than in wild-type cells (Fig. 3H). Similarly, RU360 treatment shortened the time to elevate the ratio (Fig. 3H). We also immunoblotted LC3 whose conversion from I to II marks an early autophagy stage. Again, we found MCU KO cells expedited this step compared to wild-type cells (Fig. 3I). These data demonstrate an increased mitophagy speed when MCU is inhibited and suggests that MCU-mediated mitochondrial Ca^{2+} uptake slows mitophagy kinetics.

3.5. Mitophagy-inducer-triggered mitochondrial calcium influx is faster in iPSC-derived neurons from a PD patient

To reveal mitochondrial Ca^{2+}dynamics during mitophagy initiation in human neurons, we utilized iPSCs from one familial PD patient (PD-SNCA-A53T) with the A53T mutation in *SNCA* (encodes a-synuclein) and its isogenic WT control (isogenic-WT).[14–17,33] We differentiated iPSCs to dopaminergic neurons expressing TH as previously described[14–17,33] (Fig. 4A). These PD neurons displayed mildly increased reactive oxygen species (ROS) levels measured by MitoNeoD[34] (Fig. 4B) and normal mitochondrial membrane potential detected by TMRM staining in the cell bodies (Fig. 4C). We applied Antimycin A to these neurons to trigger mitophagy as previously shown,[14–16,33] and immediately live measured mitochondrial Ca^{2+} levels by Rhod-2 staining as in Fig. 1. We found that in PD neurons mitochondrial Ca^{2+} influx was faster, with a shorter time to reach Fmax (Fig. 4D) despite similar maximum uptake (Fmax/F0) as control (Fig. 4E). We had previously shown that mitophagy was delayed in these PD neurons.[14–17,33] To probe whether targeting mitochondrial Ca^{2+} uptake could promote mitophagy, we treated these neurons with RU360 to inhibit MCU and live recorded Mito-dsRed in axons as described in.[17] The intensity reduction of mitochondrial matrix-targeted Mito-dsRed upon Antimycin A treatment indicates mitochondrial degradation via mitophagy.[14–17,33] Indeed, Mito-dsRed degradation in PD neurons was slower and RU360 treatment accelerated it (Fig. 4F). This data suggests that a faster mitochondrial Ca^{2+} import during mitophagy initiation might decelerate mitophagy in PD neurons.

4. Discussion

Our results reveal that mitochondrial Ca^{2+} uptake is a response to induction of different autophagy processes. During the first phase of mitophagy, mitochondrial Ca^{2+} import requires MCU (Fig. 3). Intriguingly, when mitochondrial Ca^{2+} uptake is inhibited in MCU KO cells or by RU360, mitophagy is expedited (Figs. 3–4). These results suggest that mitochondria may import Ca^{2+} to limit mitophagy speed, preventing over-activating mitophagy. Further investigation is warranted to explore this possibility. Cytosolic and ER Ca^{2+} signals have been shown to be essential for autophagy.[1–4] These data highlight the importance of mitochondria for fine-tuning autophagy through Ca^{2+} communications with other organelles and the cytosol (Fig. 4G).

We have previously shown that mitophagy is delayed and MCU channel activity is enhanced due to binding to Fe^{2+} in iPSC-derived neurons from PD patients.[14–17,33] Here we reveal upon mitophagy induction mitochondrial Ca^{2+} influx is faster and inhibiting MCU may promote mitophagy in these PD neurons (Fig. 4). These observations could partially explain the mitophagy defect in PD. Abnormal mitochondrial Ca^{2+} dynamics may also affect Ca^{2+}-binding proteins that play a role in mitophagy, such as PINK1, LRRK2, and Miro.[5–10,16,17] Together, these factors may contribute to the mitophagy impairment in PD neurons and eventually render cell death. Our data corroborate the concept that targeting mitochondrial Ca^{2+} transport or mitophagy is a promising strategy for neurodegenerative diseases such as PD.[35–37]

Consent to participate

Our study does not involve any human subjects. All authors consent to the publication of this paper.

Ethics approval

No human subjects or rodent models were used in this study. The iPSC work was approved by Stanford Stem Cell Oversight Committee.

Declaration of interests

The authors declare the following competing interests: X.W. is a co-founder and shareholder of AcureX Therapeutics, and a shareholder of Mitokinin Inc. The remaining authors declare no competing interests.

CRediT authorship contribution statement

Sujyoti Chandra: Writing – review & editing, Writing – original draft, Methodology, Formal analysis, Data curation. **Parul Katiyar:** Data curation. **Aarooran S. Durairaj:** Writing – review & editing, Methodology, Formal analysis, Data curation. **Xinnan Wang:** Writing – review & editing, Writing – original draft, Visualization, Validation, Supervision, Resources, Project administration, Methodology, Investigation, Funding acquisition, Conceptualization.

Acknowledgements

We thank M.F. Tsai for MCU KO cells, and V. Bharat for technical support. This work was supported by NIGMS (RO1GM143258; X.W.).

References

1. Zheng Q, Chen Y, Chen D, et al. Calcium transients on the ER surface trigger liquid-liquid phase separation of FIP200 to specify autophagosome initiation sites. *Cell*. Oct 27 2022;185(22):4082–4098.
2. MacVicar TD, Mannack LV, Lees RM, Lane JD. Targeted siRNA screens identify ER-to-mitochondrial calcium exchange in autophagy and mitophagy responses in RPE1 cells. *Int J Mol Sci*. Jun 11 2015;16(6):13356–13380.
3. Decuypere JP, Kindt D, Luyten T, et al. mTOR-controlled autophagy requires intracellular Ca(2+) signaling. *PLoS One*. 2013;8(4), e61020.
4. Bootman MD, Chehab T, Bultynck G, Parys JB, Rietdorf K. The regulation of autophagy by calcium signals: do we have a consensus? *Cell Calcium*. Mar 2018;70:32–46.
5. Apicco DJ, Shlevkov E, Nezich CL, et al. The Parkinson's disease-associated gene ITPKB protects against alpha-synuclein aggregation by regulating ER-to-mitochondria calcium release. *Proc Natl Acad Sci U S A*. Jan 5 2021;118(1).
6. Tabata Y, Imaizumi Y, Sugawara M, et al. T-Type calcium channels determine the vulnerability of dopaminergic neurons to mitochondrial stress in familial Parkinson disease. *Stem Cell Rep*. Nov 13 2018;11(5):1171–1184.
7. Buttner S, Faes L, Reichelt WN, et al. The Ca2+/Mn2+ ion-pump PMR1 links elevation of cytosolic Ca(2+) levels to alpha-synuclein toxicity in Parkinson's disease models. *Cell Death Differ*. Mar 2013;20(3):465–477.
8. Surmeier DJ, Obeso JA, Halliday GM. Selective neuronal vulnerability in Parkinson disease. *Nat Rev Neurosci*. Jan 20 2017;18(2):101–113.

9. Angelova PR, Choi ML, Berezhnov AV, et al. Alpha synuclein aggregation drives ferroptosis: an interplay of iron, calcium and lipid peroxidation. *Cell Death Differ*. Oct 2020;27(10):2781–2796.
10. Verma M, Callio J, Otero PA, Sekler I, Wills ZP, Chu CT. Mitochondrial calcium dysregulation contributes to dendrite degeneration mediated by PD/LBD-Associated LRRK2 mutants. *J Neurosci*. Nov 15 2017;37(46):11151–11165.
11. Baughman JM, Perocchi F, Girgis HS, et al. Integrative genomics identifies MCU as an essential component of the mitochondrial calcium uniporter. *Nature*. Jun 19 2011;476(7360):341–345.
12. Palty R, Silverman WF, Hershfinkel M, et al. NCLX is an essential component of mitochondrial Na+/Ca2+ exchange. *Proc Natl Acad Sci U S A*. Jan 5 2010;107(1): 436–441.
13. Kim JW, Yin X, Jhaldiyal A, et al. Defects in mRNA translation in LRRK2-mutant hiPSC-derived dopaminergic neurons lead to dysregulated calcium homeostasis. *Cell Stem Cell*. Oct 1 2020;27(4):633–645. e637.
14. Hsieh CH, Li L, Vanhauwaert R, et al. Miro1 marks Parkinson's disease subset and Miro1 reducer rescues neuron loss in Parkinson's models. *Cell Metabol*. Dec 3 2019; 30(6):1131–1140. e1137.
15. Hsieh CH, Shaltouki A, Gonzalez AE, et al. Functional impairment in Miro degradation and mitophagy is a shared feature in familial and sporadic Parkinson's disease. *Cell Stem Cell*. Dec 1 2016;19(6):709–724.
16. Shaltouki A, Hsieh CH, Kim MJ, Wang X. Alpha-synuclein delays mitophagy and targeting Miro rescues neuron loss in Parkinson's models. *Acta Neuropathol*. Oct 2018;136(4):607–620.
17. Bharat V, Durairaj AS, Vanhauwaert R, et al. A mitochondrial inside-out iron-calcium signal reveals drug targets for Parkinson's disease. *Cell Rep*. Dec 26 2023;42 (12), 113544.
18. Byers B, Cord B, Nguyen HN, et al. SNCA triplication Parkinson's patient's iPSC-derived DA neurons accumulate alpha-synuclein and are susceptible to oxidative stress. *PLoS One*. 2011;6(11), e26159.
19. Kriks S, Shim JW, Piao J, et al. Dopamine neurons derived from human ES cells efficiently engraft in animal models of Parkinson's disease. *Nature*. Dec 22 2011;480 (7378):547–551.
20. Wichterle H, Lieberam I, Porter JA, Jessell TM. Directed differentiation of embryonic stem cells into motor neurons. *Cell*. Aug 9 2002;110(3):385–397.
21. Nguyen HN, Byers B, Cord B, et al. LRRK2 mutant iPSC-derived DA neurons demonstrate increased susceptibility to oxidative stress. *Cell Stem Cell*. Mar 4 2011;8 (3):267–280.
22. Munson MJ, Mathai BJ, Ng MYW, et al. GAK and PRKCD are positive regulators of PRKN-independent mitophagy. *Nat Commun*. Oct 20 2021;12(1):6101.
23. Xiong N, Xiong J, Jia M, et al. The role of autophagy in Parkinson's disease: rotenone-based modeling. *Behav Brain Funct*. Mar 15 2013;9:13.
24. Mitter SK, Song C, Qi X, et al. Dysregulated autophagy in the RPE is associated with increased susceptibility to oxidative stress and AMD. *Autophagy*. 2014;10(11): 1989–2005.
25. Narendra D, Tanaka A, Suen DF, Youle RJ. Parkin is recruited selectively to impaired mitochondria and promotes their autophagy. *J Cell Biol*. Dec 1 2008;183(5): 795–803.
26. Clapham DE. Calcium signaling. *Cell*. Dec 14 2007;131(6):1047–1058.
27. Dong Z, Shanmughapriya S, Tomar D, et al. Mitochondrial Ca(2+) uniporter is a mitochondrial luminal redox sensor that augments MCU channel activity. *Mol Cell*. Mar 16 2017;65(6):1014–1028. e1017.
28. Ashrafi G, de Juan-Sanz J, Farrell RJ, Ryan TA. Molecular tuning of the axonal mitochondrial Ca(2+) uniporter ensures metabolic flexibility of neurotransmission. *Neuron*. Feb 19 2020;105(4):678–687. e675.
29. Aryal SP, Xia M, Adindu E, Davis C, Ortinski PI, Richards CI. ER-GCaMP6f: an endoplasmic reticulum-targeted genetic probe to measure calcium activity in astrocytic processes. *Anal Chem*. Feb 1 2022;94(4):2099–2108.
30. Suzuki J, Kanemaru K, Ishii K, Ohkura M, Okubo Y, Iino M. Imaging intraorganellar Ca2+ at subcellular resolution using CEPIA. *Nat Commun*. Jun 13 2014;5:4153.
31. Garcia-Rivas Gde J, Carvajal K, Correa F, Zazueta C. Ru360, a specific mitochondrial calcium uptake inhibitor, improves cardiac post-ischaemic functional recovery in rats in vivo. *Br J Pharmacol*. Dec 2006;149(7):829–837.
32. Young Mp, Schug Zt, Booth Dm, et al. Metabolic adaptation to the chronic loss of Ca (2+) signaling induced by KO of IP(3) receptors or the mitochondrial Ca(2+) uniporter. *J Biol Chem*. Jan 2022;298(1), 101436.
33. Li L, Conradson DM, Bharat V, et al. A mitochondrial membrane-bridging machinery mediates signal transduction of intramitochondrial oxidation. *Nat Metab*. Sep 9 2021.
34. Shchepinova MM, Cairns AG, Prime TA, et al. MitoNeoD: a mitochondria-targeted superoxide probe. *Cell Chem Biol*. Oct 19 2017;24(10):1285–1298. e1212.
35. Fang EF, Hou Y, Palikaras K, et al. Mitophagy inhibits amyloid-beta and tau pathology and reverses cognitive deficits in models of Alzheimer's disease. *Nat Neurosci*. Mar 2019;22(3):401–412.
36. Aman Y, Schmauck-Medina T, Hansen M, et al. Autophagy in healthy aging and disease. *Nat Aging*. Aug 2021;1(8):634–650.
37. Fleming A, Bourdenx M, Fujimaki M, et al. The different autophagy degradation pathways and neurodegeneration. *Neuron*. Mar 16 2022;110(6):935–966.